

NANO EXPRESS

Open Access



Research on the Preparation and Spectral Characteristics of Graphene/TMDs Hetero-structures

Tao Han , Hongxia Liu^{*}, Shulong Wang, Shupeng Chen and Kun Yang

Abstract

The Van der Waals (vdWs) hetero-structures consist of two-dimensional materials have received extensive attention, which is due to its attractive electrical and optoelectronic properties. In this paper, the high-quality large-size graphene film was first prepared by the chemical vapor deposition (CVD) method; then, graphene film was transferred to SiO₂/Si substrate; next, the graphene/WS₂ and graphene/MoS₂ hetero-structures were prepared by the atmospheric pressure chemical vapor deposition method, which can be achieved by directly growing WS₂ and MoS₂ material on graphene/SiO₂/Si substrate. Finally, the test characterization of graphene/TMDs hetero-structures was performed by AFM, SEM, EDX, Raman and PL spectroscopy to obtain and grasp the morphology and luminescence laws. The test results show that graphene/TMDs vdWs hetero-structures have the very excellent film quality and spectral characteristics. There is the built-in electric field at the interface of graphene/TMDs heterojunction, which can lead to the effective separation of photo-generated electron-hole pairs. Monolayer WS₂ and MoS₂ material have the strong broadband absorption capabilities, the photo-generated electrons from WS₂ can transfer to the underlying *p*-type graphene when graphene/WS₂ hetero-structures material is exposed to the light, and the remaining holes can induced the light gate effect, which is contrast to the ordinary semiconductor photoconductors. The research on spectral characteristics of graphene/TMDs hetero-structures can pave the way for the application of novel optoelectronic devices.

Keywords: Graphene/WS₂, Graphene/MoS₂, Hetero-structures, Raman spectrum, Photoluminescence spectrum

Introduction

The size of traditional silicon-based metal oxide semiconductor (CMOS) transistors become smaller with increase in the chip integration, and the preparation processes of device become much more complicated, so researchers have begun to focus on the ultra-thin hetero-structure-based optoelectronics [1, 2]. The two-dimensional (2D) hetero-structures can be combined by the weak van der Waals (vdWs) force between the layers and the strong covalent bond of the layer. The layers can be separated by breaking the weak van der Waals bond and then

easily transferred to other substrates [3]. The formation of new atomic-level 2D vdWs hetero-structures can be achieved by stacking the different 2D materials, and the synergistic effects of 2D hetero-structures become very important. Meanwhile, there are charge rearrangements and structural changes between adjacent crystals in hetero-structures, which can be regulated by adjusting the relative orientation of each element material. The different hetero-structures can not only maintain the properties of single material, but also produce the new physical characteristics under the synergy effect [4–6]. The vdWs hetero-structures are the material guarantee for exploring the new physical phenomena and laws, which can provide more possibilities for the nano-electronic devices with excellent photoelectric properties.

*Correspondence: hxliu@mail.xidian.edu.cn

Key Laboratory for Wide-Bandgap Semiconductor Materials and Devices of Education, the School of Microelectronics, Xidian University, Xi'an 710071, China

Since the 2D-crystalline materials have the strong interactions against a light, they have attracted extensive attentions as photosensitive materials [7]. Graphene is the atomic-level 2D material with excellent electrical, optical and mechanical properties, which has the wide application in the optoelectronics field [8–10]. However, the defect of zero band gap limits the application and development of graphene. The structure of 2D transition metal dichalcogenide (TMDs) materials is similar to that of graphene, and its band gap width changes with the layer number and thickness [11, 12]. The TMDs and graphene materials with complementary advantages are superimposed together, which can promote the application of graphene and TMDs materials in the photoelectric detection field [13–15]. The high mobility of graphene can ensure the rapid response of device, and the Van Hof singularity in electronic state density of TMDs materials ensures the strong interaction between light and materials, which can effectively enhance the absorption of light and the generation of electron–hole pairs [16, 17]. The 2D hetero-structures were widely used in the new electronic and optoelectronic devices, which is due to its transport characteristics of charge tunneling or charge accumulation, flexible energy band engineering and unique interlayer exciton characteristics. Therefore, the interlayer synergy interaction between graphene and TMDs materials can effectively control the band structure, magnetic properties and the exciton properties of hetero-structures. The graphene/TMDs hetero-structures have the high photosensitivity and light response performance, which is due to the strong quantum confinement effect [18, 19]. At present, there are the few studies on the controllable preparation methods of the large-area, large-size and high-quality graphene/TMDs hetero-structures. And the preparation processes of hetero-structures are complicated, which is still a big

challenge in terms of repeatability and controllability [20, 21]. In addition, it is difficult to understand and grasp the spectral characteristics of graphene/TMDs hetero-structures, which largely hinder the application of graphene/TMDs hetero-structures in future optoelectronic devices [22].

In this paper, graphene/WS₂ and graphene/MoS₂ hetero-structures were composed of three kinds of semiconductor materials with different dielectric constant, band gap width and absorption coefficient. The 2D materials were directly grown on the single crystal graphene film of SiO₂/Si substrate to form the graphene/TMDs hetero-structures, which can ensure the clean interface and atomic level transition of hetero-structures. The structure of graphene, MoS₂ and WS₂ can be analyzed by the AFM, SEM, EDX, Raman and photoluminescence spectroscopy to master the spectral characteristics of graphene/TMDs hetero-structures, which can be used to prepare the high-speed electron mobility transistors (HEMT) and photoelectric detectors [23–25].

Methods

Preparation and Movement of Graphene

The large-area, high-quality graphene film was prepared by CVD system, which is composed of the tube furnace, gas mixing system and vacuum machine. First, the copper foil with a size of 10 cm × 10 cm was placed into 1 mol/L hydrochloric acid solution for the 3 min ultrasonic cleaning. Then, it was washed with water and ethanol in turn. Subsequently, it was dried by blowing argon gas. Finally, it was inserted in the middle of the quartz tube, and we installed the system and corrected the air pressure [26] (Fig. 1).

As we all know, polycrystalline copper foil would affect the quality of graphene, it is necessary to anneal the copper foil substrate before the growth experiment of

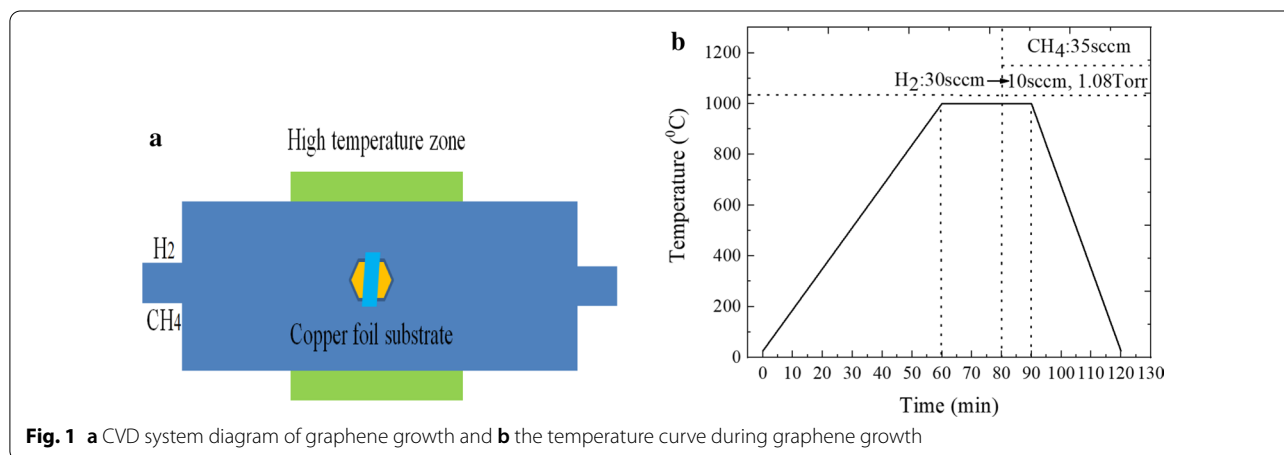


Fig. 1 a CVD system diagram of graphene growth and **b** the temperature curve during graphene growth

graphene. The specific conditions of the annealing processes at stage 1 were the following: the annealing temperature, time and the flow rate of hydrogen (H_2) gas were 1000 °C, 20 min and 30 sccm, respectively. At this time, the surface of copper foil would form the large area single crystal domain, and H_2 gas can reduce copper oxide, which can obtain the high-purity copper substrate. The growth temperature remains constant while entering stage 2, the flow rate of H_2 gas was adjusted to 10 sccm, meanwhile 35 sccm methane (CH_4) gas was also introduced, the growth time and growth pressure were, respectively, maintained for 10 min and 1.08 Torr, and the growth rate of graphene was approximately 16 $\mu\text{m/s}$ in our CVD experiment, which would ensure the preparation of relatively uniform monolayer graphene film [27, 28]. Finally, the tube furnace was quenched to room temperature at a certain rate, which can avoid damaging the surface of substrate.

The following describes the transfer-specific processes of monolayer graphene material to SiO_2/Si substrate [29]. First, PMMA solution with a mass fraction of 4% was uniformly spin-coated on the surface of monolayer graphene material with a size of 1 cm \times 1 cm, the rotation speed and time were 3000 R/min and 1 min, respectively. Next, the copper foil substrate was etched by the $(\text{NH}_4)_2(\text{SO}_4)_2$ solution with a mass fraction of 3%, and the treatment time was 3–4 h. Then, the PMMA/graphene by the glass slide was rinsed repeatedly in deionized water 2–3 times, and PMMA/graphene was removed to the 50 °C constant temperature table by SiO_2/Si substrate, which can remove the water vapor between monolayer graphene material and SiO_2/Si substrate, and the monolayer graphene material can be better attached to SiO_2/Si substrate. In this step, SiO_2/Si substrate with a size of 1 \times 1 cm² was ultrasonically cleaned with acetone, ethanol and water for 15 min, and the surface of SiO_2/Si substrate is very

clean and uniform, which is conducive to the growth of graphene/TMDs hetero-structures. Finally, PMMA/graphene/ SiO_2/Si was put in acetone solution for 3–4 h to dissolve PMMA and repeatedly wash it with alcohol and deionized water to ensure that monolayer graphene film can be transferred to SiO_2/Si substrate.

The Preparation of Graphene/TMDs Hetero-structures

In CVD dual temperature zone tube furnace, the graphene/ SiO_2/Si substrate was used for the growth of MoS_2 and WS_2 material. The MoO_3 , WO_3 and sulfur powders were used as the growth molybdenum source, tungsten source and sulfur source, respectively. The high-purity Ar gas was also used to prepare the graphene/ MoS_2 and graphene/ WS_2 hetero-structures, respectively. First, the quartz boat with 100 mg sulfur powder was placed at the upstream of tube furnace. Then, 2 mg MoO_3 powder (or WO_3 powder) was filled in another quartz boat, and the graphene/ SiO_2/Si substrate was flipped upside down on MoO_3 powder (or WO_3 powder). And then, the quartz boat equipped with the graphene/ SiO_2/Si substrate and MoO_3 powder (or WO_3 powder) was inserted into the high temperature area of tube furnace. The heating belt was wound on the quartz tube to heat the sulfur powder, which would ensure that sulfur powder was well controlled and uniformly evaporated, as shown in Fig. 2a. Next, the high-purity Ar gas with a flow rate of 50 sccm was used as carrier gas, the evaporation temperature of sulfur powder was controlled at 150 °C, the growth temperature and growth time of MoS_2 and WS_2 were 750 °C, 920 °C and 10 min, respectively. Meanwhile, the first-stage temperature was maintained at 100 °C for 10 min, which can remove the water vapor of tube furnace. The specific temperature change diagram is shown in Fig. 2b. Subsequently, sulfur powder began to sublimate to the sulfur vapor, and the sulfur vapor reaches the high

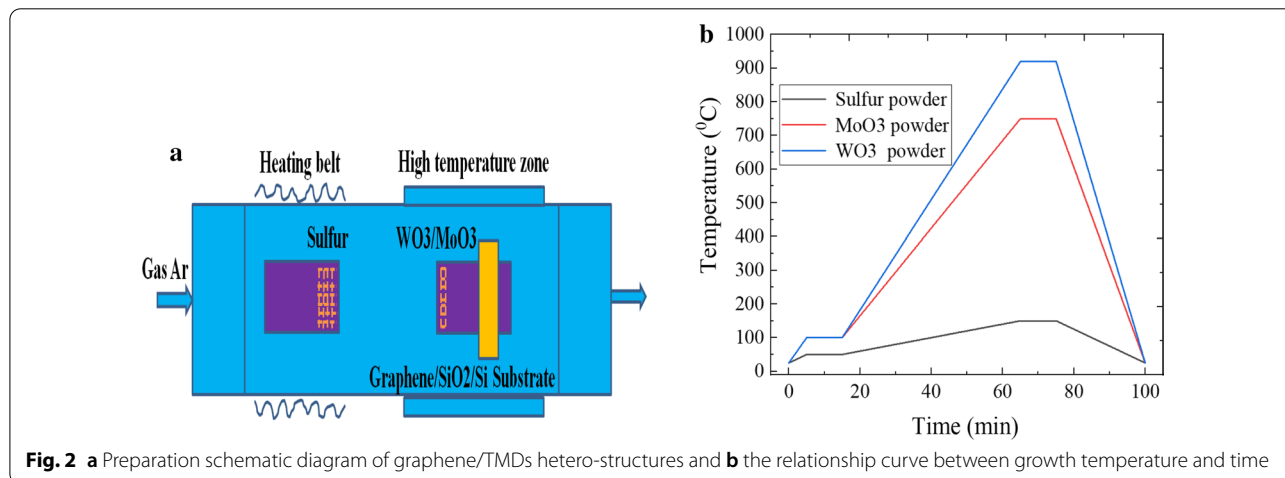


Fig. 2 a Preparation schematic diagram of graphene/TMDs hetero-structures and **b** the relationship curve between growth temperature and time

temperature area of tube furnace, which can be driven by Ar gas. It can be fully reacted with MoO_3 and WO_3 powder, and the product was deposited on graphene/ SiO_2 /Si substrate. Therefore, the growth rate of graphene/TMDs hetero-structures was consistent with that of TMDs materials [30]. After the growth of MoS_2 and WS_2 material, the tube furnace was naturally cooled to room temperature, and the color of substrate becomes light yellow.

The Test Characterization of Graphene/TMDs Hetero-structures

In this paper, the test and characterization methods of graphene/TMDs hetero-structures mainly include the optical microscope (OM), Raman and photoluminescence (PL) spectroscopy, field emission scanning electron microscope (FESEM), energy-dispersive X-ray spectroscopy (EDX) and atomic force microscope (AFM). First, the surface morphology of graphene/TMDs hetero-structures can be observed by optical microscope, SEM and AFM. The layer number of hetero-structures can be judged according to the different contrast of hetero-structure sample. Then, the spectral characteristics of graphene/TMDs hetero-structures were tested and characterized. The growth morphology, growth pattern and growth mechanism of TMDs materials on graphene surface were analyzed and speculated based on the characterization results [31]. Next, Raman spectroscopy has the advantages of quickness, high efficiency and low destructiveness in terms of characterizing 2D materials. It can directly observe the interaction of electron phonons on the sample surface, which has a very wide range of applications in 2D materials. The layer number and crystal quality of 2D materials can be effectively judged by analyzing the characteristic peak position of Raman spectra, the characteristic peak position wave number difference and other characteristics of graphene/TMDs hetero-structures. Finally, the PL spectra were also an important method for characterizing and analyzing 2D materials. When the bulk material is thinned to monolayer material, the band gap width of TMDs material changes from the indirect band gap semiconductor to the direct band gap semiconductor. Meanwhile, the fluorescence effect was significantly enhanced, and there are the obvious characteristic peaks in the PL spectra. However, if the crystal quality of graphene/TMDs hetero-structures was not high, the characteristic peak intensity of PL spectra would be small even if the sample has few layers or monolayer. Therefore, the layer thickness and crystal quality of sample can also be judged by PL spectra. In addition, the distribution, element type and concentration percentage of graphene/TMDs hetero-structures films can be obtained by FESEM and EDX. Meanwhile, the AFM test

was also used to grasp the surface cleanliness, roughness and material thickness of hetero-structures film samples.

Both the PL and Raman spectra were collected by the LabRAM HR Evolution high-resolution Raman spectrometer, which was produced by HORIBA Jobin Yvon (French company) [32, 33]. The range of Raman and PL spectra was 300 cm^{-1} – 3000 cm^{-1} and 550–800 nm, respectively. And the Raman and PL spectra were 10% power and 5% power, respectively. The following were the specific test conditions, spectral resolution $\leq 0.65\text{ cm}^{-1}$; spatial resolution: horizontal $\leq 1\text{ }\mu\text{m}$, vertical $\leq 2\text{ }\mu\text{m}$; 532 nm laser, 50 \times objective lens (beam spot diameter is 1.25 μm , and 100% laser power equivalent to 7500 $\mu\text{W}/\text{cm}^2$); scan time 15 s, and the cumulative number is 2.

Results and Discussion

The Optical Micrograph and Characterization of Graphene/ WS_2 Hetero-structure

The morphology of hetero-structures can be distinguished by the high-resolution microscope of Raman spectrometer. Figure 3a shows the optical microscope images of graphene/ WS_2 hetero-structure under the different locations of SiO_2 /Si substrate. Since the color of graphene film transferred to SiO_2 /Si substrate was not much different, the graphene film is relatively uniform and complete. The surface of graphene/ SiO_2 /Si substrate was clean except for a small amount of particles, which indicates the presence of better quality graphene film. Meanwhile, the nucleation density of WS_2 became maximum when the gas concentration is sufficient in the growth experiment of WS_2 . And the WS_2 grown on graphene/ SiO_2 /Si substrate was the triangular structure grain with the uniform grain surface and a side length about 120 μm . The shape of WS_2 was regular and complete, and the thickness was uniform, which is much larger than the size of mechanical peeling sample [34]. In Fig. 3b, since the fluorescence intensity of WS_2 sample is highly uniformly distributed, the triangular monolayer WS_2 film has the higher quality and lower defects. It can be seen from Fig. 3c, d that the morphology of WS_2 film sample is triangle, and the thickness of WS_2 film is 0.83 nm, which indicates the preparation of monolayer WS_2 film. In addition, SEM was also used to analyze the morphology of WS_2 sample film, and the morphology was the regular triangular with uniform thickness, as shown in Fig. 3e. In Fig. 3f, the dock element, sulfur element and carbon element are shown in EDX spectrum, which shows that graphene/ WS_2 hetero-structure material is successfully transferred and prepared.

The molecular vibration and rotation information of material can be obtained by Raman spectroscopy, which are the fingerprint vibration spectra for identifying the material structure. The layer number and crystal quality

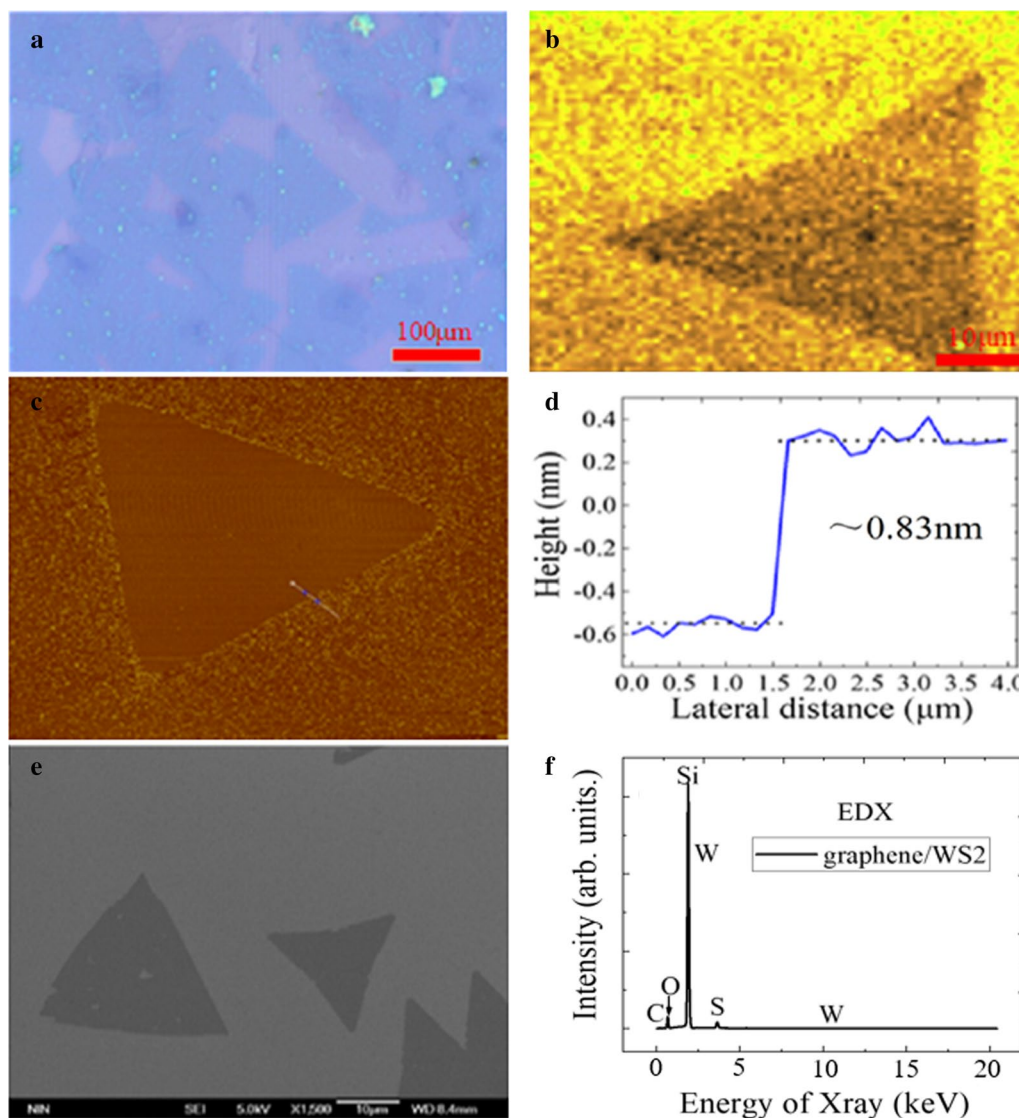
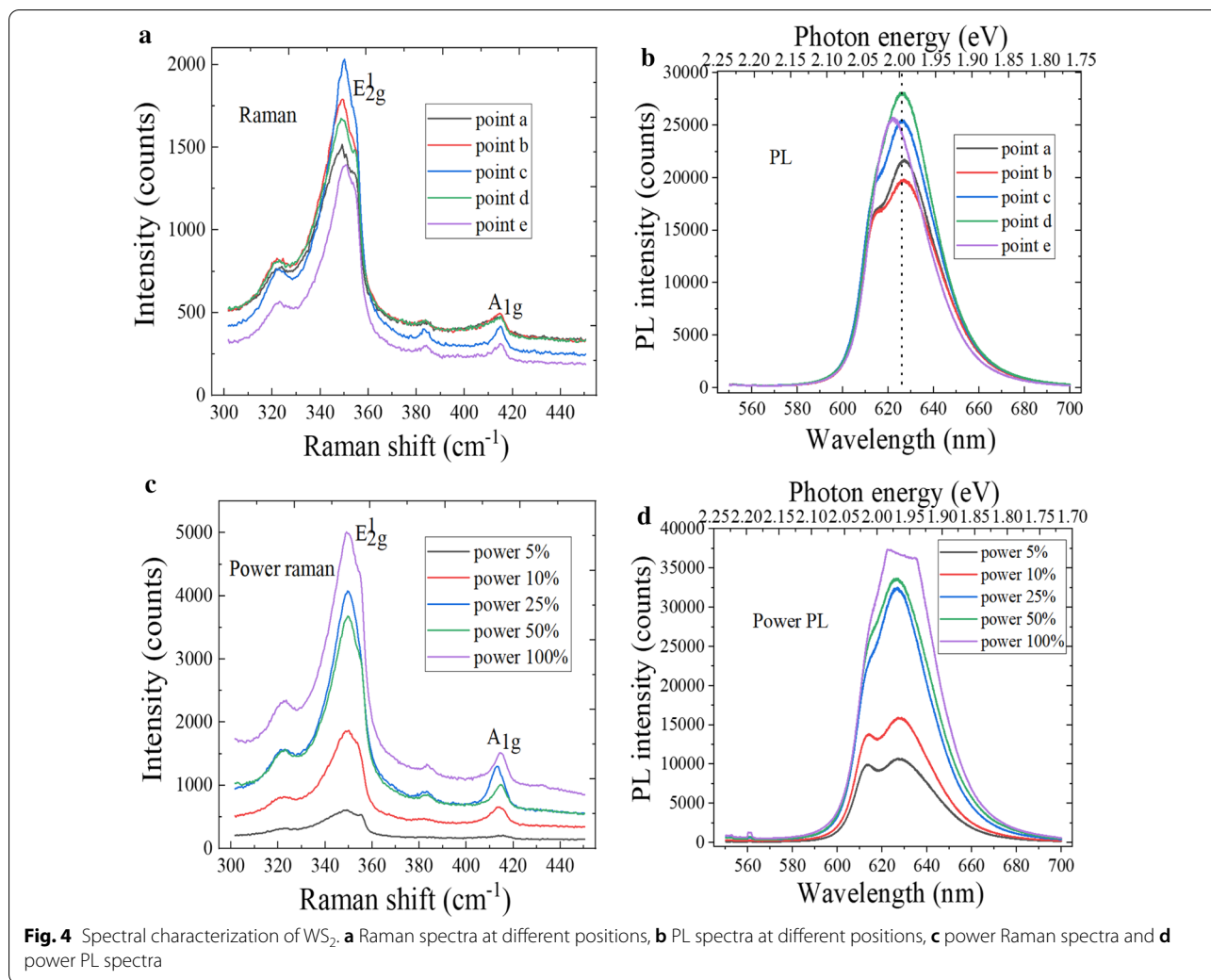


Fig. 3 **a** Optical micrograph, **b** mapping image, **c** AFM image, **d** height profile image, **e** FE-SEM image and **f** EDX spectrum of graphene/WS₂ hetero-structures on SiO₂/Si substrate

of WS₂ sample can be effectively judged by the characteristic peak position and wave number difference of Raman spectra. Figure 4a shows the Raman spectra of WS₂ sample at different positions, the E_{2g}¹ and A_{1g} characteristic peaks were located at 350.4 cm⁻¹ and 416.1 cm⁻¹, respectively. When the bulk WS₂ changes to monolayer material, E_{2g}¹ and A_{1g} characteristic peaks appear the blue-shifted and red-shifted, respectively. Therefore, the layer number can be judged by the wave numbers difference between two characteristic peaks, and the wave-number difference was 65.7 cm⁻¹, so the triangular WS₂ grains were monolayer material. In Fig. 4b, the strongest luminescence peak was located at 626 nm, and the

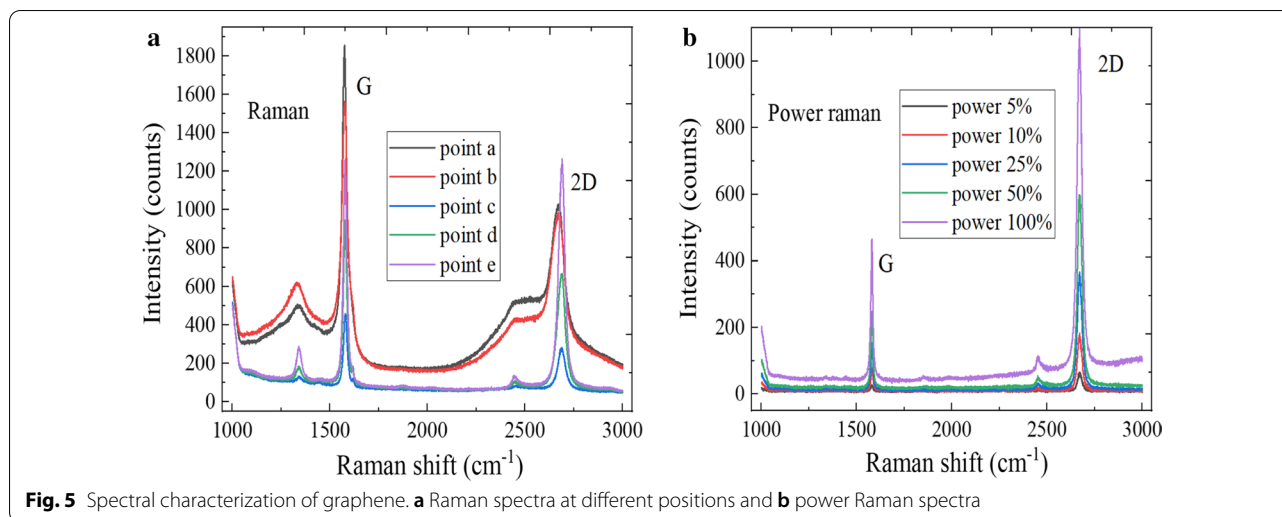
corresponding band gap was 1.98 eV, which is consistent with the band gap width of monolayer WS₂. As we all know, the PL intensity of 2D material is related to the crystal quality and layer number. The 2D material has the fewer defect and layer number, and the luminous intensity is higher, which indicates that the crystal quality is better [35]. The variable power characterization can be performed at the nW level to prevent the laser irradiation from damaging the sample. It can be found by observing Fig. 4c that the peak position of E_{2g}¹ plane vibration mode remains basically unchanged with increase in the excitation power, and the A_{1g} vibration mode between the planes moves to the short wave number direction.



This is because the A_{1g} vibration mode has the great relationship with electron concentration, and the increase in electron concentration would lead to the reformation of band gap. As shown in Fig. 4d, the PL spectra intensity of WS₂ increases with the laser power increases, and there exists the fluorescence quenching phenomenon, which is due to the reformation of band gap and the interlayer interaction of hetero-structures. At the same time, it can also be found that the local temperature of material did nearly not change with increase in the laser power. This is because WS₂ is the atomic layer-level nanomaterial.

The layer number characterization and quality information of graphene material can be obtained by Raman spectroscopy. In Fig. 5a, the Raman diffraction spectra of graphene at different positions has the three main characteristic peaks, D peak, G peak and 2D peak, were, respectively, located at 1330 cm⁻¹, 1583 cm⁻¹ and 2674 cm⁻¹. The D peak is related to the disorder of graphene lattice structure, and the position of D peak was blue-shifted

when graphene material has more lattice defects, which can reflect the defects and impurity content of crystal. The 2D peak is the two-phonon second-order resonance Raman peak, which can indicate the carbon atoms arrangement of graphene material. Besides, the G peak is caused by the E_{2g} mode of first Brillouin zone center, the peak height increases almost linearly with the layers number of graphene, and the G peak intensity is related to the doping of graphene to a certain extent. The relative ratio of 2D peak and G peak can be used to roughly determine the layers number of graphene, and the ratio of D peak to G peak would decrease when the defect density is increased. The weak D peak appears in the Raman spectra of graphene when the growth of MoS₂ (or WS₂) material was completed, which indicates that the graphene domain still maintains the high quality. The 2D peak intensity of exposed graphene area weakened, which is affected by the high-temperature growth process. The full width at half maxima (FWHM) of graphene

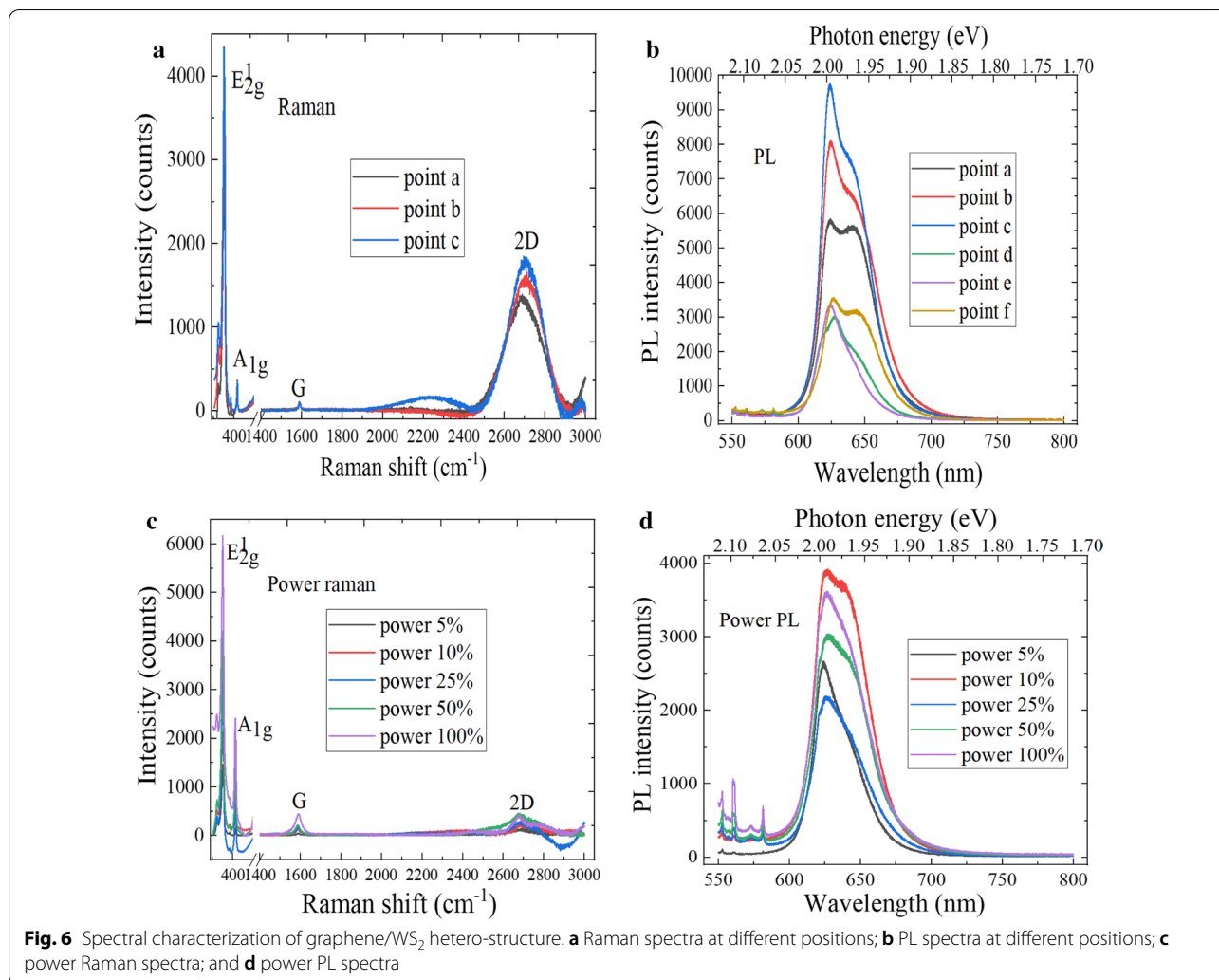


2D peak gradually increases with increase in the layers number, and the peak position of 2D peak is blue-shifted, which may be related to the energy band relationship of graphene material. The electronic energy band structure splits with increase in the layers number, and a variety of phonon resonance scattering processes would occur. The exciton peak would be excited by absorbing more energy, which would lead to the blue shift of 2D peak position. The peak intensity of G peak at Point C and E is significantly higher than that of 2D peak. The I_{2D}/I_G ratio decreases with increase in the thickness, and the transferred graphene in this experiment was not very uniform, which is within the allowable range. Figure 5b shows the power Raman spectra of monolayer graphene. The G and 2D peak intensity of graphene is gradually increasing with increase in the laser power and temperature, and there is basically no change of the peak position and FWHM. The G peak and 2D peak were, respectively, located at 1581 cm^{-1} and 2672 cm^{-1} , and the intensity of two characteristic peaks differs greatly. Due to the interaction change between graphene and underlying SiO_2 , the characteristic peak ratio of I_{2D}/I_G is decreased. Meanwhile, there were no D defect peak of Raman spectra, which indicate that the selected graphene region has a high quality and the carbon atoms are highly ordered.

Raman spectroscopy was used to characterize and analyze the graphene/ WS_2 hetero-structure material, and there were two spectra of $300\text{ cm}^{-1} \leq \omega \leq 500\text{ cm}^{-1}$ and $1400\text{ cm}^{-1} \leq \omega \leq 3000\text{ cm}^{-1}$, which were fitted by the Lorentz function. There were the E_{2g}^1 and A_{1g} modes characteristic peaks of WS_2 in the range of $300\text{ cm}^{-1} \leq \omega \leq 500\text{ cm}^{-1}$. The E_{2g}^1 phonon mode is the in-plane displacement of sulfur and tungsten atoms, while the A_{1g} phonon mode is the out-of-plane displacement of sulfur atoms, the above phonon mode locations

and intervals vary with the layers number. The G and 2D peaks of graphene appear in the spectra region of $1400\text{ cm}^{-1} \leq \omega \leq 3000\text{ cm}^{-1}$, and the layer number and crystal quality information of graphene can be obtained according to the intensity ratio and the peak position of characteristic peaks.

The frequency difference of two different Davydov splitting peaks can reflect the interaction magnitude of vdWs hetero-structures. Therefore, the intra-layer vibrating phonon mode frequency of multilayer 2D material also depends on the interlayer coupling and layers number. Figure 6a shows the Raman spectra test characterization of graphene/ WS_2 hetero-structure at different points under the 532 nm laser. It can be found that the intensity of E_{2g}^1 characteristic peak was higher than that of A_{1g} characteristic peak intensity, and the E_{2g}^1 and A_{1g} characteristic peaks were located at 349.3 cm^{-1} and 417.1 cm^{-1} , respectively. The Raman spectra 2D and G peaks of graphene/ WS_2 hetero-structure were, respectively, at 1591.5 cm^{-1} and 2680.9 cm^{-1} , and the peak position of 2D and G peaks rise compared with pure graphene, which may be related to the effective interlayer coupling of WS_2 nano-sheets and the strain effect generated by the high temperature heating during CVD growth. The Raman spectra of graphene/ WS_2 hetero-structure material is only the sum of the individual separated WS_2 and graphene spectra, which can confirm the formation of vdWs heterojunction interface. The PL spectra intensity is related to the crystal quality and layer number. Raman spectroscopy focuses on the influence of hetero-structures formation on the vibration modes, and the electronic band structure of TMDs hetero-structures material can be mainly obtained by PL spectra. Figure 6b shows the PL spectra of graphene/ WS_2 hetero-structure at different points. The strongest luminescence peak was



located at 624 nm, and the corresponding band gap was 1.99 eV, which is consistent with the band gap width of monolayer WS_2 . The graphene/ WS_2 hetero-structure material at different positions has the different intensity and shape of PL spectra, and the crystal quality is not very good. Therefore, the preparation processes of hetero-structure need to be further improved. The PL spectra intensity of graphene/ WS_2 hetero-structure is weaker than that of WS_2 . This is because the inter-layer coupling of graphene/ WS_2 hetero-structure changes the exciton fluorescence of hetero-structures region, which would lead to the separation of electron-hole pairs and the reduction in fluorescence. Meanwhile, the peak position shifts when the graphene/ WS_2 hetero-structure is formed, and the transfer of charge can cause the shift of Fermi surface, which can make the free excitons change into the charged excitons. Figure 6c shows the power Raman spectra of graphene/ WS_2 hetero-structure. The in-plane phonon mode E_{2g}^1 characteristic peak and the

out-of-plane phonon mode A_{1g} characteristic peak were, respectively, at 356 cm^{-1} and 418 cm^{-1} , where the above characteristic peak is increased with increase in the laser power. The peak position and shape of characteristic peak were uniform within single crystal, and the electronic characteristics of WS_2 on graphene/ SiO_2/Si substrate were uniform. The thickness of WS_2 sheet can be determined according to the frequency difference between A_{1g} and E_{2g}^1 characteristic peaks, and the average distance was $62 \pm 0.2\text{ cm}^{-1}$, which is consistent with the thickness of monolayer WS_2 . Compared to the peak positions of intrinsic graphene, the G peak and 2D peak positions of graphene/ WS_2 hetero-structure from 1578.7 cm^{-1} and 2685.8 cm^{-1} change to 1582.2 cm^{-1} and 2689.5 cm^{-1} , respectively. Besides, the intensity of G peak becomes stronger than that of 2D peak with increase in the laser power, and decrease in the I_{2D}/I_G ratio, which is caused by the interaction change between graphene and SiO_2/Si substrate [36, 37]. It can be found by observing Fig. 6d

that the PL intensity of graphene/WS₂ hetero-structure is increased with increase in the laser power, the FWHM of PL spectra also increasing, and the shape of PL spectra is changed. The reason is that the test temperature around hetero-structure is increased, and there is also the strong interlayer coupling at the interface of graphene/WS₂ heterojunction.

The Raman spectra of graphene/WS₂ hetero-structure were significantly different from that of exposed graphene region, as shown in Fig. 7a. First, the spectral background rises when wavenumber increases, and the background comes from the PL spectra of WS₂, which confirms the presence of graphene/WS₂ hetero-structure. Next, WS₂ material can suppress the 2D characteristic peak intensity of graphene. Finally, both G peak and 2D peak of graphene/WS₂ hetero-structure shift upward compared with the spectra of bare graphene material. Due to the interlayer coupling between graphene and WS₂, the 2D peak would also shift up, and the mechanical strain also has the impact on the Raman shift of graphene. The enhancement factor (EF) is the ratio of the maximum peak intensity of graphene/WS₂ hetero-structure divided by the maximum peak intensity of graphene. The maximum peak intensity of G peak increases from 460 to 830, and the maximum peak intensity of 2D peak increases from 340 to 1460, and the corresponding EF were 1.8 and 4.3, respectively. The D peak signal is significantly enhanced when the graphene/TMDs hetero-structures is formed. Therefore, the I_D/I_G ratio of monolayer graphene is weaker than that of graphene/WS₂ hetero-structure. This is because the extrusion of WS₂ on graphene has the effect on the structure of graphene, which would result in the appearance of a small number of defects. In Fig. 7b, the PL intensity of graphene/WS₂ hetero-structure is higher than that of bare graphene, which may be

related to the effective interlayer coupling and the strain effect. Meanwhile, the maximum intensity of PL spectra is increased from 270 to 1410, and the corresponding EF is 5.23. The intensity enhancement of characteristic peak can be attributed to the coupling of graphene/WS₂ hetero-structure.

Raman spectroscopy can be used to evaluate the crystal quality and film thickness of 2D materials. The Raman spectra comparison of WS₂ and graphene/WS₂ hetero-structure is shown in Fig. 8a. Compared to the Raman spectra of WS₂, the A_{1g} mode characteristic peak position of graphene/WS₂ hetero-structure was blue-shifted, and the intensity of E_{2g}¹ mode and A_{1g} mode characteristic peaks was higher than those of WS₂, and the graphene/WS₂ hetero-structure film has the excellent crystallinity. The reason is that the coupling between layers can be enhanced when the two materials are stacked to form the hetero-structure, which would generate the interlayer interaction forces. The maximum E_{2g}¹ and A_{1g} characteristic peak intensity increases from 3400 and 1100 to 6500 and 2950, respectively. And the enhancement factors (EF) are 1.9 and 2.7, respectively. In addition, monolayer WS₂ and multilayer WS₂ are the direct band gap semiconductor and indirect semiconductor materials, respectively. Therefore, the PL spectroscopy can be used to identify the layer number of WS₂ sample. In Fig. 8b, the above two materials show that the strongest PL emission was around 626 nm, and that the band gap was approximately at 1.98 eV, which is consistent with band gap of the mechanically peeled monolayer WS₂. The PL intensity of graphene/WS₂ hetero-structure was stronger than that of monolayer WS₂. The reasons are the following: First, the work function between graphene and WS₂ does not match. Second, the internal field was formed. Third, the photoelectrons from WS₂ can transfer to graphene.

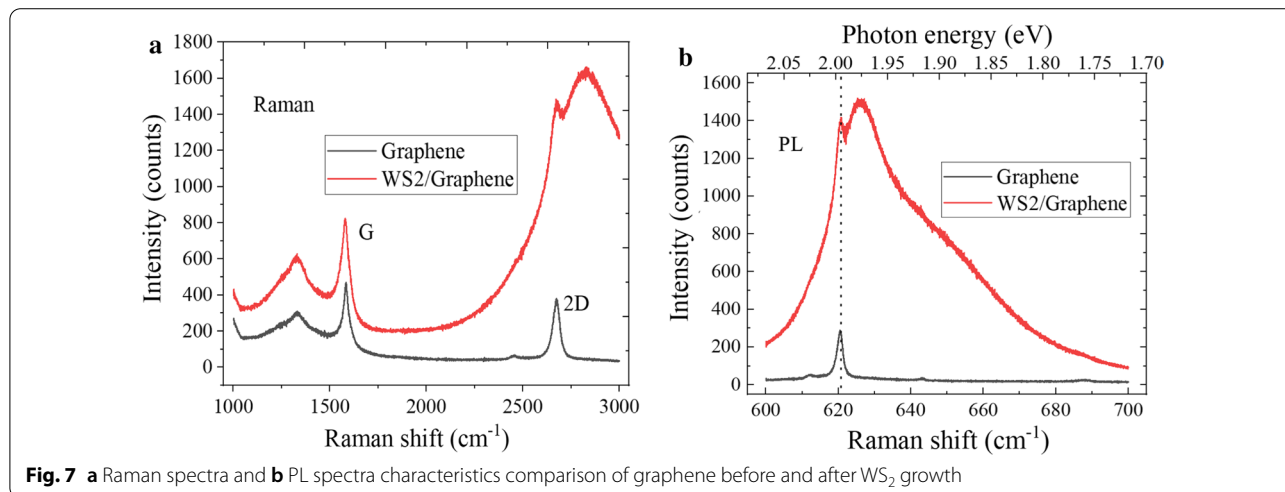
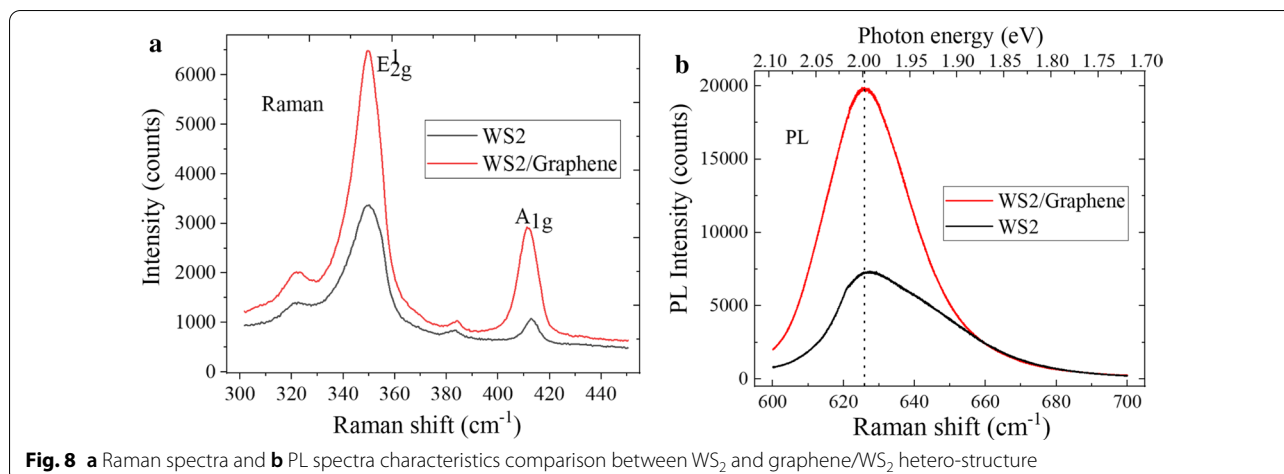


Fig. 7 a Raman spectra and b PL spectra characteristics comparison of graphene before and after WS₂ growth



Forth, the WS₂ material retains holes. The maximum intensity of strongest peak increases from 7450 to 19,320, and the EF of PL spectra are 2.6. The increase in peak intensity is due to the coupling between graphene and WS₂ materials.

Optical Micrograph and Characterization of Graphene/MoS₂ Hetero-structure

The optical microscope pictures of graphene/MoS₂ hetero-structure on SiO₂/Si substrate are shown in Fig. 9a. We found that the color of the graphene transferred to SiO₂/Si substrate was not much different from the original one. The surface was relatively clean except for a few particles in some areas. These results indicate that the graphene film is uniformly and completely formed. The MoS₂ thin film covers graphene/SiO₂/Si substrate, which can be connected into the continuous graphene thin film across the grain boundaries. The prepared graphene/MoS₂ hetero-structure was continuous and intact, and the sample surface was relatively clean, which has the good surface uniformity. The local fluorescence intensity distribution is not uniform when there are many defects. Figure 9b shows the in-plane fluorescence intensity distribution of triangular monolayer MoS₂ film. The crystal lattice of sample has the fewer defects. In Fig. 9c, d, the surface condition of the material is observed by AFM, and the height difference between the edge of the material and the graphene/SiO₂/Si substrate is measured to judge the material thickness, the thickness of monolayer MoS₂ material is about 0.81 nm. It can be found by the SEM test result that the morphology of MoS₂ film sample is the triangular flake, as shown in Fig. 9e. It can be found by observing Fig. 9f that the molybdenum, sulfur and carbon elements are uniformly distributed in the EDX spectrum, which indicates that the graphene/MoS₂ hetero-structure has been successfully prepared.

The interlayer interaction weakens with decrease in the film thickness. The A_{1g} mode characteristic peak is red-shifted, whereas the characteristic peak of E_{2g}¹ mode is blue-shifted. As a result, the frequency distance between A_{1g} and E_{2g}¹ vibration modes becomes smaller, which can be used to identify the thickness of 2D materials. Figure 10a shows the Raman spectra of MoS₂ at different positions. The characteristic peaks of E_{2g}¹ mode and A_{1g} mode were at 381.2 cm⁻¹ and 400.5 cm⁻¹, respectively. And the peak spacing was 19.3 cm⁻¹, which indicates the presence of monolayer MoS₂. Due to the Van der Waals force between the layers, the frequencies of two vibration modes moving in the same or opposite directions between adjacent atoms in the layers are slightly different. The PL spectra are used to obtain the light emission characteristics of MoS₂ film, as shown in Fig. 10b. As we all know, the luminous intensity of monolayer MoS₂ was much greater than that of multilayer, and the electronic band structure changed from indirect band gap to direct band gap when the layer number of MoS₂ material changed from multilayer to single layer. Therefore, there was only the strong emission peak of monolayer MoS₂. In addition, the strongest PL peak was at 678.5 nm, and the corresponding direct band gap was 1.83 eV, which is close to the band gap value of mechanically peeling MoS₂ film. It can be found by observing Fig. 10c that the characteristic peak intensity of Raman spectra is increased with increase in the laser power and that the peak positions of E_{2g}¹ and A_{1g} mode characteristic peak were blue-shifted. This is because the Raman peak line would have a certain frequency shift with increase in the temperature and laser power. Figure 10d shows the power PL spectra of MoS₂, the luminous intensity increasing accordingly with increase in the laser power, and the strongest PL peak position was blue-shifted.

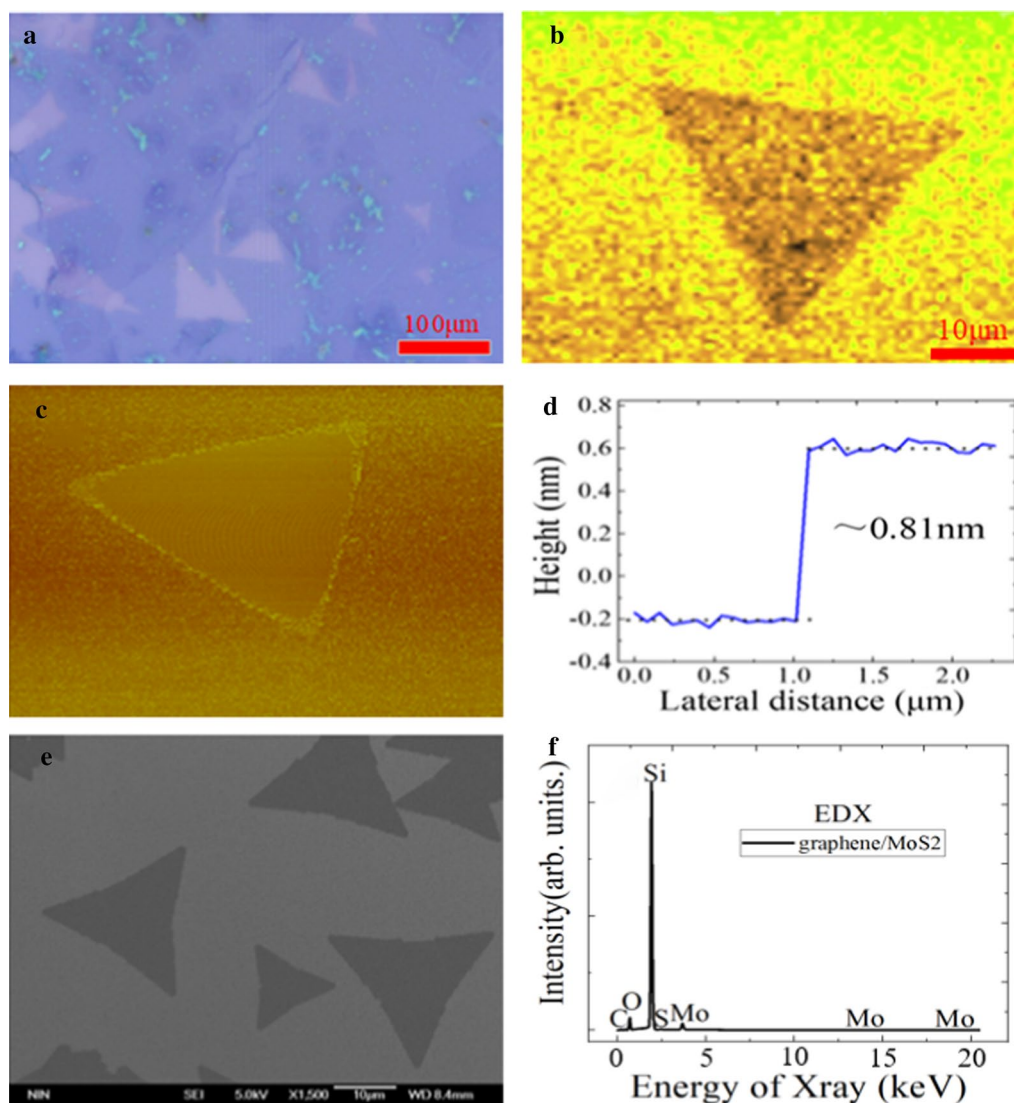
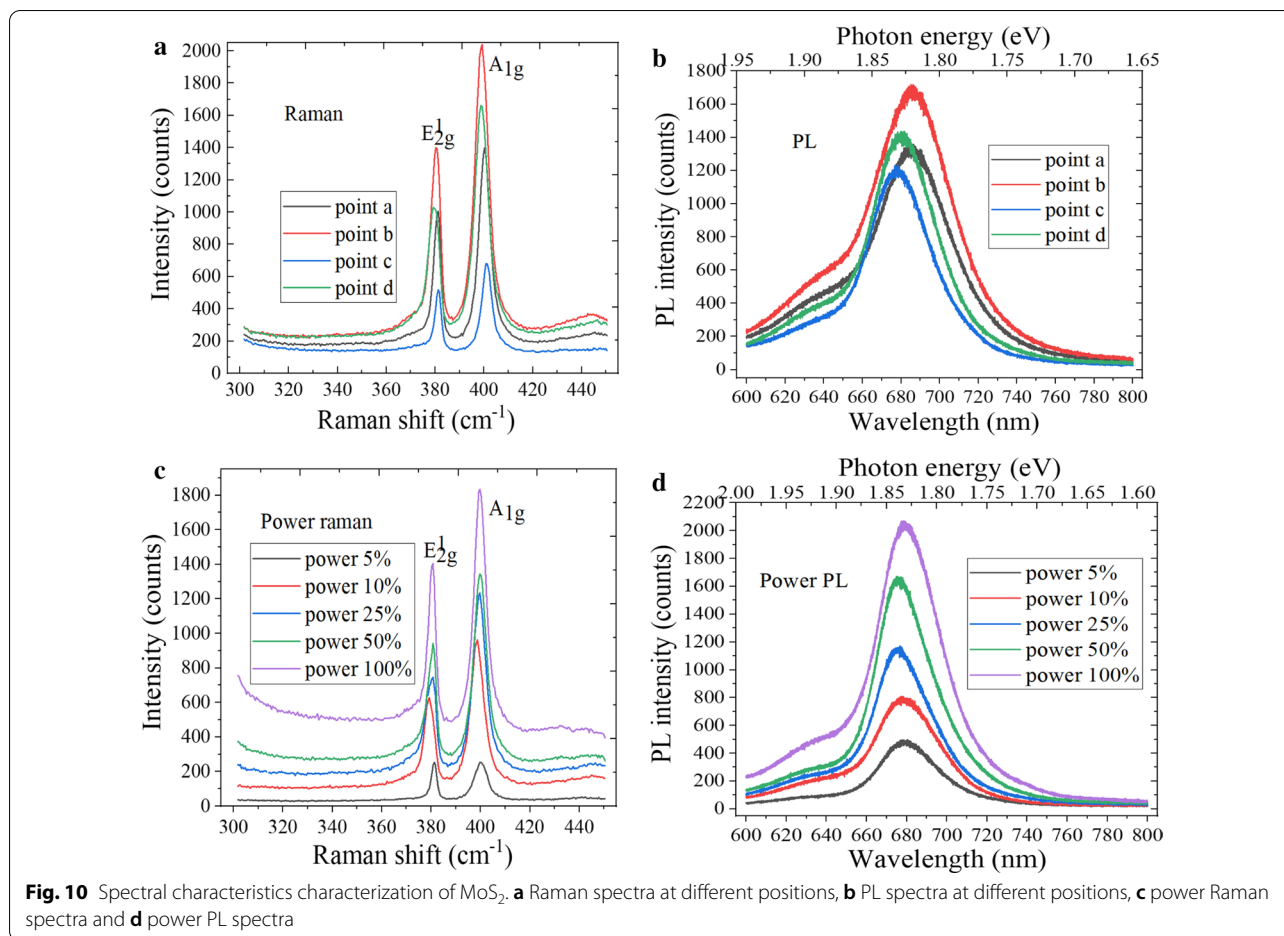


Fig. 9 **a** Optical micrograph, **b** mapping image, **c** AFM image, **d** height profile image, **e** FE-SEM image and **f** EDX spectrum of graphene/MoS₂ hetero-structure on SiO₂/Si substrate

A high-frequency layer vibrating phonon mode of monolayer 2D material would split into the N corresponding high-frequency modes in an N-layer 2D material, which would lead to the Davydov splitting. Figure 11a shows the Raman spectra of graphene/MoS₂ hetero-structure, and there were the G, 2D peaks of graphene and the E_{2g}¹ and A_{1g} peaks of MoS₂, which indicates the formation of layered graphene/MoS₂ hetero-structure material. The E_{2g}¹ and A_{1g} Raman characteristic peaks of MoS₂ were located at 375.5 cm⁻¹ and 394.4 cm⁻¹, respectively. And the peak spacing was 18.9 cm⁻¹. Compared with intrinsic graphene, the G peak and 2D peak positions of graphene/MoS₂ hetero-structure shift to large wavenumbers, and

G peak and 2D peak move from 1581 and 2672 cm⁻¹ to 1587 and 2674 cm⁻¹, respectively. In addition, the intensity of G peak is stronger than that of 2D peak. The rise of the 2D and G peaks position is related to the effective interlayer coupling and the strain effect. Compared with the Raman spectra of MoS₂ material, the spectra of graphene/MoS₂ hetero-structure material are significantly shifted due to the enhancement of interlayer atomic interaction, and the peak intensity can also be significantly enhanced. It can be found from Fig. 11b that the graphene/MoS₂ hetero-structure has two absorption peaks at 621 nm and 683 nm and that the corresponding band gaps were 1.99 eV and 1.82 eV according to the



conversion relationship between wavelength and electron volt. The luminous intensity of graphene/MoS₂ hetero-structure was lower than that of intrinsic MoS₂. The reasons of these phenomena are that the graphene material has the weakening effect on the fluorescence of MoS₂ material and that the electronic energy band and electronic distribution can be changed due to the interlayer coupling, which can greatly change the PL and Raman spectra.

Figure 11c shows the power Raman spectra of graphene/MoS₂ hetero-structure, the Raman peaks intensity of G, 2D, E_{2g}¹, and A_{1g} increasing with increase in the laser power. The peak position difference between E_{2g}¹ and A_{1g} is gradually enhanced with increase in the layer number of MoS₂ material. The characteristic peak positions of E_{2g}¹ and A_{1g} were 377.2 cm⁻¹ and 396.7 cm⁻¹, respectively. And the peak position difference was 19.5 cm⁻¹, which can be judged that MoS₂ material is the monolayer. Meanwhile, the G and 2D peaks of graphene were red-shifted and blue-shifted, respectively. This is because graphene material is doped with MoS₂. It can be found by observing Fig. 11d that there were two

PL peaks of graphene/MoS₂ hetero-structure. These PL peak corresponding to the compound transition of A and B excitons, wherein the light emission corresponding to the direct band gap exciton recombination was 1.84 eV, whereas the peak corresponding to the indirect band gap exciton recombination was at 2.0 eV. The luminous intensity of strongest peak is increased with increase in the laser power, and the peak position of the strongest PL spectra is red-shifted. This is due to the *p*-type conductivity of the graphene and the change of band structure when graphene and MoS₂ materials were stacked. In addition, the arrangement of energy bands at the interface allows the electrons from electron-rich MoS₂ to transfer to *p*-type graphene material.

Conclusion

Graphene/TMDs-based hetero-structures, where WS₂ and MoS₂ were used as TMDs material, were successfully synthesized directly on graphene films by using APCVD. The morphology, spectral characteristics and luminescence law of hetero-structures can be obtained by AFM, SEM, EDX, Raman and PL spectroscopy, and

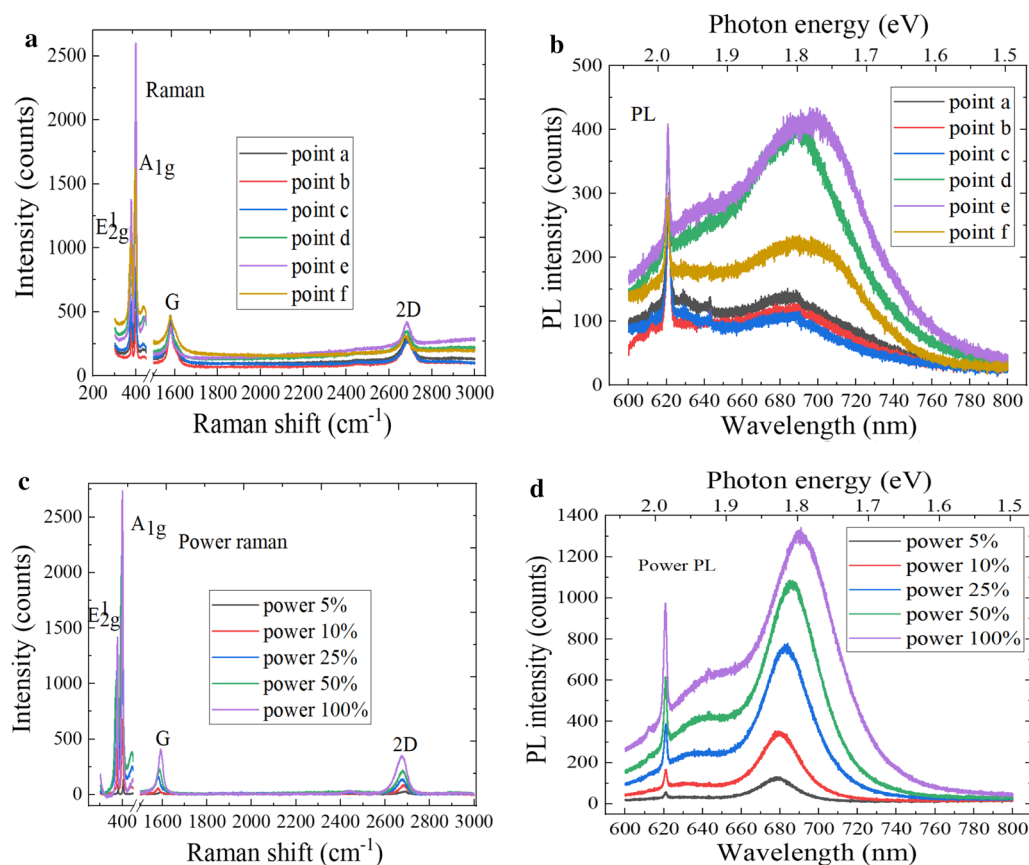


Fig. 11 Spectral characteristics of graphene/MoS₂ hetero-structure. **a** Raman spectra at different positions, **b** PL spectra at different positions, **c** power Raman spectra and **d** power PL spectra

the hetero-structures show the excellent photosensitivity. Compared with intrinsic graphene material, the G and 2D peak positions of graphene/TMDs hetero-structures are the blue-shifted, the intensity of G peak is stronger than that of 2D peak with increase in the laser power and decrease in the I_{2D}/I_G ratio. Due to the presence of internal electric field, the photo-generated electron-hole pairs can be effectively separated at the interface of graphene/TMDs hetero-structures, which could greatly improve the light response. This research could effectively guide the preparation process improvement in large-area, high-quality hetero-structures, and it could also pave the way for the application of graphene/TMDs hetero-structures in the optoelectronic devices field.

Abbreviations

2D TMDs: Two-dimensional transition-metal dichalcogenides; vdWs: Van der Waals; HEMT: High-speed electron mobility transistors; PMMA: Polymethyl methacrylate; MoS₂: Molybdenum disulfide; APCVD: Atmospheric pressure chemical vapor deposition; WO₃: Molybdenum trioxide; OM: Optical microscopy; PL: Photoluminescence; MoO₃: Molybdenum trioxide.

Acknowledgements

TH and KY are Ph.D. students in Xidian University. SpC is a doctor in Xidian University. SIW is an associate professor in Xidian University. HxL is a professor in Xidian University.

Authors' contributions

TH generated the research idea, analyzed the data, and wrote the paper. TH, KY and SC carried out experiments. TH and KY participated in the discussion. SW and HL have given the final approval of the version to be published. All authors read and approved the final manuscript.

Funding

This research was funded by the National Natural Science Foundation of China (Grant No. U1866212), the Laboratory Open Fund of Beijing Smart-chip Microelectronics Technology Co., Ltd. (Grant No. SGITZDDKJQT2002303), the Innovation Foundation of Radiation Application (Grant No. KFZC2018040206). This research was also supported by SixCarbon Technology Shenzhen.

Availability of data and materials

The experiment data supporting the conclusion of this manuscript have been given in this manuscript.

Competing interests

The authors declare that they have no competing interests.

Received: 8 June 2020 Accepted: 26 October 2020
Published online: 25 November 2020

References

- Sun D, Ye D, Liu P, Tang Y, Guo J, Wang L, Wang H (2018) MoS₂/Graphenenanosheets from commercial bulky MoS₂ and graphite as anode materials for high rate sodium-ion batteries. *Adv Energy Mater* 8(10):1702383
- Thanh TD, Chuong ND, Van Hien H, Kshetri T, Kim NH, Lee JH (2018) Recent advances in two-dimensional transition metal dichalcogenides-graphene hetero-structures materials for electrochemical applications. *Progress Mater Sci* 96:51–85
- Yuan L, Chung TF, Kuc A, Wan Y, Xu Y, Chen YP, Heine T, Huang L (2018) Photocarrier generation from interlayer charge-transfer transitions in WS₂-graphene hetero-structures. *SciAdv* 4(2):e1700324
- Tian H, Liu M, Zheng W (2018) Constructing 2D graphitic carbon nitride nanosheets/layered MoS₂/graphene ternary nanojunction with enhanced photocatalytic activity. *ApplCatal B Environ* 225:468–476
- Wang R, Wang S, Jin D, Zhang Y, Cai Y, Ma J, Zhang L (2017) Engineering layer structure of MoS₂-graphene composites with robust and fast lithium storage for high-performance Li-ion capacitors. *Energy Storage Mater* 9:195–205
- Yamaguchi T, Moriya R, Inoue Y, Morikawa S, Masubuchi S, Watanabe K, Taniguchi T, Machida T (2014) Tunneling transport in a few monolayer-thick WS₂/graphene hetero-structures. *ApplPhysLett* 105(22):223109
- Liu Q, Cook B, Gong M, Gong Y, Ewing D, Casper M, Wu J (2017) Printable transfer-free and wafer-size MoS₂/graphene van der Waals hetero-structures for high-performance photodetection. *ACS Appl Mater Interfaces* 9(14):12728–12733
- You B, Wang X, Mi W (2015) Prediction of spin-orbital coupling effects on the electronic structure of two dimensional van der Waals hetero-structures. *PhysChemChemPhys* 17(46):31253–31259
- Murugadoss V, Wang N, Tadakamalla S, Wang B, Guo Z, Angaiah S (2017) In situ grown cobalt selenide/graphenenanocomposite counter electrodes for enhanced dye-sensitized solar cell performance. *J Mater Chem A* 5(28):14583–14594
- Zhang D, Jia Y, Cheng J, Chen S, Chai J, Yang X, Han C (2018) High-performance microwave absorption materials based on MoS₂-graphene isomorphous hetero-structures. *J Alloys Compd* 758:62–71
- Liu M, Shi J, Li Y, Zhou X, Ma D, Qi Y, Zhang Y, Liu Z (2017) Temperature-triggered sulfur vacancy evolution in monolayer MoS₂/graphene hetero-structures. *Small* 13(40):1602967
- Kirubasankar B, Palanisamy P, Arunachalam S, Murugadoss V, Angaiah S (2019) 2D MoSe₂-Ni(OH)₂ nanohybrid as an efficient electrode material with high rate capability for asymmetric supercapacitor applications. *ChemEng J* 355:881–890
- Li C, Cao Q, Wang F, Xiao Y, Li Y, Delaunay JJ, Zhu H (2018) Engineering graphene and TMDs based van der Waals hetero-structures for photovoltaic and photoelectrochemical solar energy conversion. *ChemSoc Rev* 47(13):4981–5037
- Xie Y, Chou TM, Yang W, He M, Zhao Y, Li N, Lin ZH (2017) Flexible thermoelectric nanogenerator based on the MoS₂/graphenenanocomposite and its application for a self-powered temperature sensor. *SemicondSciTechnol* 32(4):044003
- Kirubasankar B, Murugadoss V, Lin J, Ding T, Dong M, Liu H, Zhang J, Li T, Wang N, Guo Z, Angaiah S (2018) In situ grown nickel selenide on graphenenanohybrid electrodes for high energy density asymmetric supercapacitors. *Nanoscale* 10(43):20414–20425
- Liu X, Gao J, Zhang G, Zhang YW (2017) MoS₂-graphene in-plane contact for high interfacial thermal conduction. *Nano Res* 10(9):2944–2953
- Omar S, van Wees BJ (2017) Graphene-WS₂ hetero-structures for tunable spin injection and spin transport. *Phys Rev B* 95(8):081404
- Subasri A, Balakrishnan K, Nagarajan ER, Devadoss V, Subramania A (2018) Development of 2D La(OH)₃/graphenenanohybrid by a facile solvothermal reduction process for high-performance supercapacitors. *ElectrochimActa* 281:329–337
- Biroju RK, Pal S, Sharma R, Giri PK, Narayanan TN (2017) Stacking sequence dependent photo-electrocatalytic performance of CVD grown MoS₂/graphene van der Waals solids. *Nanotechnology* 28(8):085101
- Zhao Y, Zhang X, Wang C, Zhao Y, Zhou H, Li J, Jin H (2017) The synthesis of hierarchical nanostructured MoS₂/graphene composites with enhanced visible-light photo-degradation property. *Appl Surf Sci* 412:207–213
- O'Suilleabhain D, Vega-Mayoral V, Kelly AG, Harvey A, Coleman JN (2019) Percolation effects in electrolytically gated WS₂/graphenenano: nano composites. *ACS Appl Mater Interfaces* 11(8):8545–8555
- Song H, Wang B, Zhou Q, Xiao J, Jia X (2017) Preparation and tribological properties of MoS₂/graphene oxide composites. *Appl Surf Sci* 419:24–34
- Aeschlimann S, Rossi A, Chávez-Cervantes M, Krause R, Arnoldi B, Stadtmüller B, Aeschlimann M, Forti S, Fabbri F, Coletti C, Gierz I (2020) Direct evidence for efficient ultrafast charge separation in epitaxial WS₂/graphene hetero-structures. *Sci Adv* 6(20):eaay0761
- Du L, Yu H, Liao M, Wang S, Xie L, Lu X, Yang R (2017) Modulating PL and electronic structures of MoS₂/graphene hetero-structures via interlayer twisting angle. *ApplPhysLett* 111(26):263106
- Maurya DK, Balan B, Murugadoss V, Yan C, Angaiah S (2020) A fast Li-ion conducting Li_{7.1}La₃Sr_{0.05}Zr_{1.95}O₁₂ embedded electrospun PVDF-HFP nanohybrid membrane electrolyte for all-solid-state Li-ion capacitors. *Mater Today Commun* 25:101497
- O'Farrell ECT, Avsar A, Tan JY, Eda G, Ozyilmaz B (2015) Quantum transport detected by strong proximity interaction at a graphene-WS₂ van der Waals interface. *NanoLett* 15(9):5682–5688
- Antonova IV (2016) Vertical hetero-structures based on graphene and other 2D materials. *Semiconductors* 50(1):66–82
- Kirubasankar B, Vijayan S, Angaiah S (2019) Sonochemical synthesis of a 2D-2D MoSe₂/graphenenanohybrid electrode material for asymmetric supercapacitors. *Sustain Energy Fuels* 3(2):467–477
- Kim YC, Nguyen VT, Lee S, Park JY, Ahn YH (2018) Evaluation of transport parameters in MoS₂/graphene junction devices fabricated by chemical vapor deposition. *ACS Appl Mater Interfaces* 10(6):5771–5778
- Meng X, Yu L, Ma C, Nan B, Si R, Tu Y, Bao X (2019) Three-dimensionally hierarchical MoS₂/graphene architecture for high-performance hydrogen evolution reaction. *Nano Energy* 61:611–616
- Murugadoss V, Panneerselvam P, Yan C, Guo Z, Angaiah S (2019) A simple one-step hydrothermal synthesis of cobaltnickelselenide/graphenenanohybrid as an advanced platinum free counter electrode for dye sensitized solar cell. *ElectrochimActa* 312:157–167
- He J, Kumar N, Bellus MZ, Chiu HY, He D, Wang Y, Zhao H (2014) Electron transfer and coupling in graphene-tungsten disulfide van der Waals hetero-structures. *Nat Commun* 5(1):1–5
- Horri A, Faez R, Pourfath M, Darvish G (2017) A computational study of vertical tunneling transistors based on graphene-WS₂ hetero-structures. *J ApplPhys* 121(21):214503
- Kirubasankar B, Murugadoss V, Angaiah S (2017) Hydrothermal assisted in situ growth of CoSe onto graphenenanosheets as a nanohybrid positive electrode for asymmetric supercapacitors. *RSC Adv* 7(10):5853–5862
- Wang Y, Chen Y, Wu X, Zhang W, Luo C, Li J (2018) Fabrication of MoS₂-graphene modified with Fe₃O₄ particles and its enhanced microwave absorption performance. *Adv Powder Technol* 29(3):744–750
- Arunachalam S, Kirubasankar B, Murugadoss V, Vellasamy D, Angaiah S (2018) Facile synthesis of electrostatically anchored Nd(OH)₃nanorods onto graphenenanosheets as a high capacitance electrode material for supercapacitors. *New J Chem* 42(4):2923–2932
- Paradisanos I, McCreary KM, Adinehloo D, Mouchliadis L, Robinson JT, Chuang HJ, Kioseoglou G (2020) Prominent room temperature valley polarization in WS₂/graphene hetero-structures grown by chemical vapor deposition. *ApplPhysLett* 116(20):203102

Publisher's Note

Springer Nature remains neutral with regard to jurisdictional claims in published maps and institutional affiliations.